Journal of Nuclear Medicine, published on April 21, 2016 as doi:10.2967/jnumed.116.172759

^{18}F-FDG PET derived tumor blood flow changes after one cycle of neoadjuvant chemotherapy predicts outcome in triple-negative breast cancer

Olivier Humbert[1,2]; Jean-Marc Riedinger[1,3]; Jean-Marc Vrigneaud[1,2] ;Salim Kanoun[1,2,4] ; Inna Dygai-Cochet[1]; Alina Berriolo-Riedinger[1]; Michel Toubeau[1] ; Edouard Depardon[1]; Maud Lassere[1]; Simon Tisserand[1]; Pierre Fumoleau[5]; François Brunotte[1,2,4] ; Alexandre Cochet[1,2,4]

[1] Department of Nuclear Medicine, Centre GF Leclerc, Dijon, France;

[2] LE2I UMR 6306, CNRS, Arts et Métiers, Univ. Bourgogne Franche-Comté, France ;

[3] Departments of Biology and Pathology, Centre GF Leclerc, Dijon, France;

[4] Imaging Department, CHU Le Bocage, Dijon, France;

[5] Department of Medical Oncology, Centre GF Leclerc, Dijon, France;

Corresponding author: Dr. Olivier Humbert (M.D; Ph.D)

Centre GF Leclerc, 1 rue du Pr Marion, 21000 Dijon, France

Telephone: +33-3-80737522

Fax: +33-3-80737732

Email: ohumbert@cgfl.fr

Word count = 4994

The authors have no disclosure or financial support to declare.

Running title: blood flow response in breast cancer

ABSTRACT

Previous studies have suggested that early changes in blood flow (BF) in response to neoadjuvant chemotherapy and evaluated with ^{15}O-water are a surrogate biomarker of outcome in women with breast cancer. This study investigates, in the triple-negative breast cancer (TNBC) subtype, the prognostic relevance of tumor BF changes in response to chemotherapy, assessed using a short dynamic ^{18}F-FDG PET acquisition. **Methods**: Forty-six consecutive women with TNBC and an indication for neoadjuvant chemotherapy were prospectively included. Women benefited from a baseline ^{18}F-FDG PET exam with a 2-min chest-centered dynamic acquisition, started at the time of ^{18}F-FDG injection. Breast tumor perfusion was calculated from this short dynamic image using a first-pass model. This dynamic PET acquisition was repeated after the first cycle of chemotherapy to measure early changes in tumor BF (ΔBF). Delayed static PET acquisitions were also performed (90 min after ^{18}F-FDG injection) to measure changes in tumor glucose metabolism (ΔSUV_{max}). The association between tumor BF, clinico-pathological characteristics and patients' overall survival (OS) was evaluated. **Results:** Median baseline tumor BF was 21 ml/min/100g [range, 6-46 ml/min/100g] and did not significantly differ according to tumor size, SBR grade or Ki-67 expression. Median tumor ΔBF was -30% with highly scattered values [range, -93%;+118%]. A weak correlation was observed between ΔBF and ΔSUV_{max} (r=+0.40, p=0.01). The median follow-up was 30 months (range, 6-73 months). Eight women developed recurrent disease, seven of whom died. Low overall survival was associated with menopausal history (p=0.03), persistent or increased tumor vascularization on the interim PET (ΔBF cut-off = -30%; p=0.03), non-breast-conserving surgery (p=0.04) and the absence of a

pathological complete response (pCR) (p=0.01). ΔBF and pCR provided incremental prognostic stratification: 3-years OS was 100% in pCR-women; 87% in no-pCR women but achieving an early tumor BF response; and only 48% in no-pCR/no-BF response women (ΔBF cut-off=-30%, p<0.001). **Conclusion**: This study suggests the clinical usefulness of an early "user- and patient-friendly" 2-min dynamic acquisition to monitor breast tumor blood flow changes to neoadjuvant chemotherapy using ^{18}F-FDG PET/CT. Monitoring tumor perfusion and angiogenesis response to treatment seems to be a promising target for PET tracers.

Keys words: triple-negative, breast cancer, PET, blood flow, perfusion

INTRODUCTION

Breast cancer includes different molecular entities (*1*). Triple-negative breast cancers (TNBC) are defined by the lack of hormone receptor expression and no overexpression of HER2 (*2,3*). This subtype is characterized by an aggressive clinical course marked by high rates of metastases and poor outcome (*2*). Neoadjuvant chemotherapy aims to improve rates of breast conservation (*4*) but also offers an opportunity to evaluate early biomarkers of tumor response. The identification of biomarkers, either molecular or otherwise, that could distinguish between highly responsive and non-responsive tumors early is of critical importance to tailor treatments to tumor response in individual patients.

Previous studies found that early changes in tumor glucose metabolism, assessed with ^{18}F-Fluorodeoxyglucose Positron Emission Tomography/Computer Tomography (^{18}F-FDG PET/CT) after the first or second course of neoadjuvant chemotherapy, can indicate breast cancer response early (*5,6*), especially in the aggressive TNBC subtype (*7,8*).

Beyond tumor glucose metabolism, the ability to induce angiogenesis is another hallmark of cancer cells: the presence of functional vasculature is essential for the growth of solid tumors. In addition to their cytotoxic action, conventional chemotherapeutic agents exert effects on tumor vasculature, indirectly by interrupting proangiogenic support secondary to tumor cell kill and directly by affecting endothelial cell function (*9*). In the era of precision medicine, one of the challenges facing the field of tumor response monitoring is to find predictive biomarkers to identify tumors with angiogenic resistance. In such tumors, standard treatments may require the adjunction of a pure angiogenic inhibitor (*10*).

Previous studies have demonstrated that early changes in tumor blood flow (BF) measured by ^{15}O-water PET or in the flow component extracted from 1-hour-dynamic ^{18}F-FDG PET scans (K_1) were associated with pathologic tumor response and outcomes among women with locally advanced breast cancer (*11-13*); Patients with persistent or incremental increases in FDG K1 were more likely to relapse or die. Kinetic FDG measurements were found more useful than static SUV measurements (*14*);

Due to the very short half-life of ^{15}O-water, an on-site cyclotron is required and very few nuclear-medicine centers have one. Moreover ^{18}F-FDG PET kinetic analysis requires an acquisition of 1-hour. There is thus an impetus for clinically practical methods capable of estimating kinetic parameters from PET studies. Mullani et al. developed a first-pass model for the in vivo calculation of blood flow with PET. This model was applied to the evaluation of tumor blood flow using ^{18}F-FDG and demonstrated good correlations with blood flow measured with ^{15}O-water (*15*).

The present study investigated the clinical and prognostic relevance of early changes in tumor perfusion in response to neoadjuvant treatment, using baseline and interim short dynamic ^{18}F-FDG PET/CT acquisitions. We focused on women with TNBC, which is a challenging tumor subtype due to its high clinical aggressiveness.

MATERIALS AND METHODS

Patients and study design

From February 2009 to October 2014, 260 women referred to our institution for clinical stage II or III invasive breast cancer with an indication for neoadjuvant

chemotherapy were consecutively and prospectively evaluated. Only women with TNBC were included. This population overlaps those of previous articles published by our team (*7,16*). Patients with high glycemia (>9 mmol/l), unwilling to undergo the complete PET exams or with suspected metastasis on baseline ^{18}F-FDG PET were excluded. The institutional review board approved this prospective study as a current care study. The medical team documented the non opposition of the patient in source document and in the information note provided to the patient (the requirement to obtain signed consent was waived)."

Most Women underwent sequential chemotherapy with anthracyclines (FEC100, 3 courses every 3 weeks) followed by taxanes (3 courses every 3 weeks). This systematic switch was done in conformance with institutional guidelines and not based on PET response monitoring. Few of the women, included at the beginning of the study, underwent 6 cycles of FEC100. One month after the last course of chemotherapy, the tumors were surgically removed and examined by a pathologist. Radiotherapy was performed according to standard recommendations. Patients were followed up every three months during the first two years, every six months for the following three years, and then once per year.

Pathological analysis

Pre-treatment core biopsies from the primary tumor were used to determine the histological type and the tumor Scarf-Bloom-Richardson (SBR) grade (*17*). The following immunohistochemical markers were examined: estrogen receptor (ER), progesterone receptor (PR) and HER2 expression. All immunostaining was performed on an automated immunostainer (Ventana XT, Tucson). ER and PR status were considered

negative if the tumor showed less than 10% of positive cells. HER2 status was graded according to the HercepTest scoring system (*18*). In cases of 2+ scores, fluorescent in situ hybridization was used according to ASCO/CAP criteria (*18*).

Pathological complete response (pCR) was defined as no residual invasive cancer in the breast and nodes, though in-situ breast residuals were allowed (ypT0/is ypN0) (*19*).

^{18}F-FDG-PET/CT procedures

A first ^{18}F-FDG-PET scan was done at baseline. Two different PET/CT imaging systems were used: a Gemini GXL PET/CT scanner from February 2009 to December 2010 and a Gemini TF PET/CT scanner from December 2010 to October 2014 (Philips Medical Systems). Patients were instructed to fast for at least 6 hours before the intravenous injection of 5 MBq/kg of ^{18}F-FDG for Gemini GXL studies and 3 MBq/kg for Gemini TF studies.

^{18}F-FDG was injected using an automatic PET infusion system (Intego; Medrad) at a rate of 1 mL/s. Simultaneously with the injection, the first chest-centered emission acquisition with patient in the prone position, using a breast imaging coil, was run in the list mode for 2 minutes, followed by a low-dose CT scan. Reconstructions of 5 and 10-second frames were extracted from this dynamic first-pass acquisition. Sixty minutes after the ^{18}F-FDG injection, a whole-body PET scan was done. Finally, 90 min after the injection, a PET scan restricted to the chest (2 bed positions) with patients in the prone position, was performed. Emission data were corrected for dead time, random and scatter coincidences and attenuation before reconstruction with the row action maximum-likelihood algorithm.

A few days before the second course of chemotherapy, a second ^{18}F-FDG PET scan was performed with the same early dynamic first-pass acquisition and late chest-restricted PET static acquisition.

First-Pass Model for Measurement of tumor blood flow (Supplemental Fig. 1). The concept and method for measuring tumor blood flow from the first pass of ^{18}F-FDG has been explained in a previous paper from our institution (*20*). Briefly, it is based on the first-pass model of Mullani et al. (*15,21*) hypothesizing that 1) during the early period of the first transit of a highly extracted tracer through the tumor, the venous concentration of the tracer can be considered zero. 2) the first-pass extraction fraction of ^{18}F-FDG in tumor tissue is high, close to those of ^{15}O-water (*15*). 3) so as to minimize the error in flow measurement due to the statistical quality of the data, the numerator and the denominator are determined at their maximum values: this peak count time (T_m) was defined on the arterial time–activity curve as the end of the first pass of the tracer in the volume of interest (VOI) drawn inside the ascending aorta (Supplemental Fig. 1). A VOI encompassing the primary tumor was also manually drawn. Mixed functional and anatomical contouring was used to delineate the breast tumor. Tumors BF at baseline (BF1) and after the 1st cycle of chemotherapy (BF2) were then calculated in mL/min/100g of tumor, using the following equation:

$$BF = \frac{Q(T_m)}{E \times \int_0^{Tm} Ca(t)dt}$$

$Q(T_m)$ is the amount of the tracer in tumor tissue at time T_m, E is the tumor first-pass extraction fraction of ^{18}F-FDG which is assumed to be equal to 1 (*15*), Ca(t) is the arterial concentration of the tracer at time t.

The tumor blood flow response to chemotherapy was calculated:

$\Delta BF\ (\%) = 100 \times (BF_2 - BF_1) / BF_1$

Tumor glucose metabolism measurements. A spheroidal VOI encompassing the primary tumor was manually drawn on the chest-restricted acquisitions obtained at 90min after tracer injection to measure the Standardized Uptake Value maximal index at baseline ($SUV1_{max}$) and after the first course of chemotherapy ($SUV2_{max}$). Measured SUV_{max} were corrected for body surface area and glycaemia, as detailed in our previous studies (*22;23*). The metabolic response to treatment was calculated as follows:

$\Delta\ SUV_{max}\ (\%) = 100 \times (SUV2_{max} - SUV1_{max}) / SUV1_{max}$.

The ratio between baseline tumor glucose metabolism and perfusion ($SUV1_{max}/BF_1$) was calculated.

Statistical analysis

Continuous variables are expressed as medians and ranges, or means and standard deviations. The study endpoints were the oncological outcomes of relapse-free survival and overall survival (OS). Relapse-free survival was defined as the time from date of breast cancer diagnosis (biopsy) until the first evidence of disease recurrence (local, regional or distant). Alive patients without progression were censored at the last follow-up. OS was defined as the time from diagnosis until the date of death or, if alive, the date of the last clinical follow-up.

The Pearson's correlation coefficient (r) between ΔSUV_{max} and ΔBF was calculated. Receiver operating characteristic curves (ROC) were used to compare the predictive values for pCR.

Univariate cox proportional-hazards models were calculated to compute the hazard ratios (HRs) with their 95% Confidence Intervals (CI). All p-values were two-sided and considered significant when no greater than 0.05.

Median follow-up with its 95% CI and survival curves were calculated using the Kaplan-Meier method. Survival outcomes were compared using log-rank tests.

WinSTAT software (Microsoft, Redmond, Washington, USA) and Systat software (Systat Inc, Evanston, IL) were used.

RESULTS

Patients' characteristics (Supplemental Table 1)

Among the 260 women evaluated, 57 (22%) had TNBC. Eleven women were then excluded: one of them because of uncontrolled glycaemia, five because of unexpected stage IV upstaging, 5 because the first-pass dynamic acquisitions was not performed for different reasons (technical problems, refusal…). In the remaining 46 patients finally included in the study, 6 missed the second PET scan.

Patient's characteristics are detailed in Supplemental Table 1. Briefly, the median age was 46 years (range, 26-85 years). The median primary tumor size, assessed with breast ultrasound and/or mammogram, was 3.6 cm (range, 1.5-6.7cm). On ultra-sound scan, 32/46 women had lymph node involvement (based on sonographic features of the lymph nodes). Almost all the tumors were invasive ductal carcinoma (45/46) and one was an invasive lobular carcinoma.

The median value of tumor BF_1 was 21 ml/min/100g [range, 6-46 ml/min/100g]. Neither tumor size, SBR grade, mitotic count nor ki-67 tumor expression were associated with BF_1 values and the $SUV1_{max}/BF_1$ ratio;

Median tumor ∆BF was -30% [range, -93%;+118%]. Thirty percent of the women (12/40) experienced increased tumor blood flow after the first cycle of treatment.

Compared to ∆BF, median tumor ΔSUV_{max} showed less scattered values (median ΔSUV_{max}= -50.0% [range, -87;+15%]). A weak correlation was observed between ΔSUV_{max} and ΔBF (r=+0.40; p=0.01) (Fig. 1).

The mean timeframe between interim PET and surgery was 19 weeks (standard deviation= 2 weeks). Conservative surgery was performed in 65% (30/46) of the women. The pCR rate was 43% (20/46). Using ROC curve analyses, ΔSUV_{max} predicted pCR with an area under the curves (AUC) of 0.82±0.07 (p=0.0007), whereas ΔBF did not reach significance (AUC= 0.66±0.09; p=0.09).

Survival analysis (Fig. 2; Table 1)

The median follow-up period was 30 months (range, 6-73 months). Eight of the 46 women included developed recurrent disease, seven of whom died. The 3-year relapse-free survival rate was 77.3% (95% CI=[62.9%-91.7%]) and the 3-year OS rate was 82.2% (95%CI =[69.0%-95.4%]).

Continuous variables were dichotomized according to their median value. Univariate Cox analysis for OS demonstrated that menopausal history, no significant decrease in tumor blood flow after the first cycle of chemotherapy (ΔBF cut-off = -30%) and non-breast-conserving surgery were associated with worst OS (p=0.035, 0.037 and 0.046

respectively) (Table 1). Women who died had an average increase in tumor ΔBF (+11.6 ± 56%), whereas those who survived had an average decrease (-30.4 ± 45%). Given the small number of events, the multivariate analysis was not performed.

The Kaplan-Meier curves for OS with dichotomized values of ΔBF, type of surgery following NAC and histological tumor response are shown in Figure 2. Women achieving a pCR had excellent outcome (3-year OS = 100%). In women who did not achieved a pCR, tumor ΔBF could further stratify between women with good or poor-outcome: 3-years OS was 87.5% in no-pCR women but who did experienced an early tumor ΔBF decrease, whereas OS was only 48.5% in women who neither achieved a pCR nor an ΔBF response (ΔBF cut-off=-30%; $p<0.001$).

DISCUSSION

Angiogenesis plays an important role in both growth and metastasis of many cancers and is thus recognized as one of the main hallmarks of oncogenesis (*24*). In TNBC, the association of an antiangiogenic agent (bevacizumab) with conventional neoadjuvant chemotherapy, increases the pCR rate (*25*) but without any survival benefit demonstrated (*26*) emphasizing the need for biomarkers of the angiogenic cascade, to better select women who may benefit from antiangiogenic drugs.

Several imaging modalities, which yield different imaging-derived hemodynamic parameters, have been proposed for the non-invasive assessment of tumor vascularity and the response to treatment (*27*). In the neoadjuvant setting of breast cancer, these modalities demonstrated that maintained tumor BF at therapy mid-point was associated

with poorer survival (*12,13*). Dynamic contrast-enhanced MRI (DCE-MRI) is widely available and frequently used in studies evaluating tumor BF response to treatment (*28,29*). DCE-MRI-derived biomarkers, particularly those involving tumor kinetic textures, are able to predict tumor histological response early (*28,29*). The clinical value of monitoring tumor blood flow using ^{15}O-water PET has also been evaluated: BF in breast cancer is highly variable and women with persistent or elevated tumor BF on interim PET experienced poorer tumor response and outcomes (*11-13*), thus paralleling our results in the specific TNBC population. Using pharmacokinetic modeling, the flow component extracted from 1-hour-dynamic ^{18}F-FDG PET imaging (K_1) yields a good correlation to ^{15}O-water PET and DCE-MRI-measured blood-flows of breast cancer (*30,31*). In the neoadjuvant setting, FDG-K_1 changes over the first course of treatment provide the same prognostic information as BF changes assessed with ^{15}O-water PET (*13*).

One main limitation of all these previous studies was that they evaluated tumor blood flow in all breast cancer subtypes pooled together. Today, this is less relevant than a per-subtype analysis due to the well-known molecular heterogeneity of breast cancer entities (*1,32*). Other limitations are that, ^{15}O-water PET requires an on-site cyclotron and that ^{18}F-FDG-PET kinetic complete analysis requires a long and uncomfortable acquisition procedure for the patient (1 hour). Further optimization of ^{18}F-FDG kinetic analysis measurements are needed to yield insights into practical alternatives that overcome the limitations of purely static measurements.

To assess tumor blood flow, we applied a dynamic first-pass model developed by Mullani et al., based on a simple 1-compartment flow model. This model estimates blood

flow using only the first 2 min of data after injection. This short dynamic acquisition is suitable for routine practice (*15,21*). Tumor blood flow assessed with this model is linearly correlated with ^{15}O-water-measured blood flow (r=0.86) (*15*) and with breast tumor angiogenesis as measured by immunohistochemistry markers (*20*).

Using this first-pass model, we evaluated early tumor BF changes in response to chemotherapy in the challenging and aggressive TNBC subtype. Our estimated TNBC blood flow at baseline averaged 21 ml/min/100g, which agrees with previous reports using ^{15}O-water PET (*11,30,31*). The tumor blood flow response (ΔBF) showed highly scattered values, ranging from -93% to +118%, which weakly correlated with tumor metabolic changes (r=0.4). Patients whose tumors failed to show a significant decrease in tumor BF after the 1st cycle of treatment (ΔBF cut-off= -30%) had a higher risk of recurrence and death. These results are consistent with those of Dunnwald et al., obtained in all tumor subtypes pooled together and using ^{15}O-water PET and dynamic ^{18}F-FDG PET (*13,14*).

In TNBC, pCR at the end of neoadjuvant chemotherapy has been demonstrated a crucial endpoint: women who do not achieve it have a higher risk of relapse and reduced overall survival (*19*). We found a 100% 3-year overall survival in women reaching a pCR. The more accurate exclusion of oligometastatic women by the baseline ^{18}F-FDG PET exam, compared with previous studies using conventional imaging, may explain the excellent prognostic stratification of the pCR as already shown by Groheux et al. (*33*).

Contrary to ΔSUV_{max}, ΔBF was not a good predictor of pCR. But interestingly, ΔBF and pCR seemed to provide incremental prognostic stratification in the TNBC subtype: 3-years OS was 100% in pCR-women; 87% in no-pCR women but achieving an early

tumor BF response; and only 48% in no-pCR/no-BF response women. We could thus identify a very high-risk subgroup of women who neither experienced an early tumor BF decrease after introducing chemotherapy nor a pCR at the end of treatment. This study may thus be an important step towards the use of ^{18}F-FDG-PET to quantify different aspects of tumor biology and their changes in response to therapy, using a single ^{18}F-FDG injection and two short PET acquisitions (early dynamic for tumor BF and late static for tumor glucose metabolism).

Our study has some limitations. First, TNBC is a rare subtype, which explains the small cohort of women: the results are preliminary. Secondly, the simple 1-compartment flow model used in this study has some intrinsic limitations, already described (*15*). Briefly, the first pass of ^{18}F-FDG imaging may contain a few trapped components of ^{18}F-FDG that can lead to an overestimation of BF. On the other hand, the first-pass extraction of ^{18}F-FDG, relative to the ^{15}O-water, averaged 0.86, thus suggesting a small underestimation of BF (*15*). Furthermore, the limited count statistic arising from a short static acquisition has statistical fluctuation that may impact the results.

Persistent cancer-cell derived cytokines may explain the persistent or increased tumor blood flow in resistant tumors after initiating neoadjuvant chemotherapy (*34*). But our results leave questions unanswered about the relationship between preserved tumor BF during treatment and the higher likelihood of metastatic failure. The elevated level of tumor BF after initiating treatment may directly facilitate the spread of tumor metastatic cells via the circulation (*35*), or may be a consequence of a more invasive TNBC phenotype which could withstand cancer treatment and metastasize. The use of functional imaging modalities in combination with tissue based genomic profiling will

offer a unique opportunity to elucidate the critical biological pathways that underlie our results. Molecular imaging also holds promises for in-vivo imaging of tumor angiogenesis with the development of new specific probes, for example against integrin (*36*).

CONCLUSION

This study showed that patients with breast carcinoma exhibiting persistent or even increased tumor vascularization after the first cycle of neoadjuvant chemotherapy experienced worse outcomes. Its great interest lies in the fact that it focused on the particularly aggressive TNBC subtype and demonstrated the prognostic usefulness of an early “user- and patient-friendly” 2-min dynamic ^{18}F-FDG PET acquisition to monitor tumor blood flow changes. Imaging biomarkers of breast tumor perfusion may help the physician to better select women with TNBC who may benefit from the adjunction of angiogenic inhibitor drugs.

DISCLOSURE: The authors have no conflicts of interest or financial disclosure to declare.

ACKNOWLEDGMENTS: This study is part of the PharmImage® project. We thank Mr Bastable for proof-reading the text.

REFERENCES

1. Perou CM, Sorlie T, Eisen MB, et al. Molecular portraits of human breast tumours. *Nature.* 2000; 406:747-752.

2. Foulkes WD, Smith IE, Reis-Filho JS. Triple-negative breast cancer. *N Engl J Med.* 2010; 363:1938-1948.

3. Oakman C, Viale G, Di LA. Management of triple negative breast cancer. *Breast.* 2010; 19:312-321.

4. Fisher B, Brown A, Mamounas E, et al. Effect of preoperative chemotherapy on local-regional disease in women with operable breast cancer: findings from national surgical adjuvant breast and bowel project B-18. *J Clin Oncol.* 1997; 15:2483-2493.

5. Schwarz-Dose J, Untch M, Tiling R, et al. Monitoring primary systemic therapy of large and locally advanced breast cancer by using sequential positron emission tomography imaging with [18F]fluorodeoxyglucose. *J Clin Oncol.* 2009; 27:535-541.

6. Groheux D, Majdoub M, Sanna A, et al. Early metabolic response to neoadjuvant Treatment: FDG PET/CT criteria according to breast cancer subtype. *Radiology.* 2015; 277:358-371.

7. Humbert O, Riedinger JM, Charon-Barra C, et al. Identification of biomarkers including 18FDG-PET/CT for early prediction of response to neoadjuvant chemotherapy in triple negative breast cancer. *Clin Cancer Res.* 2015;21:5460-5468.

8. Groheux D, Hindie E, Giacchetti S, et al. Early assessment with 18F-fluorodeoxyglucose positron emission tomography/computed tomography can help predict the outcome of neoadjuvant chemotherapy in triple negative breast cancer. *Eur J Cancer.* 2014; 50:1864-1871.

9. Miller KD, Sweeney CJ, Sledge GW, Jr. Redefining the target: chemotherapeutics as antiangiogenics. *J Clin Oncol.* 2001; 19:1195-1206.

10. Lambrechts D, Lenz HJ, de HS, Carmeliet P, Scherer SJ. Markers of response for the antiangiogenic agent bevacizumab. *J Clin Oncol.* 2013; 31:1219-1230.

11. Mankoff DA, Dunnwald LK, Gralow JR, et al. Blood flow and metabolism in locally advanced breast cancer: relationship to response to therapy. *J Nucl Med.* 2002; 43:500-509.

12. Mankoff DA, Dunnwald LK, Gralow JR, et al. Changes in blood flow and metabolism in locally advanced breast cancer treated with neoadjuvant chemotherapy. *J Nucl Med.* 2003; 44:1806-1814.

13. Dunnwald LK, Gralow JR, Ellis GK, et al. Tumor metabolism and blood flow changes by positron emission tomography: relation to survival in patients treated with neoadjuvant chemotherapy for locally advanced breast cancer. *J Clin Oncol.* 2008; 26:4449-4457.

14. Dunnwald LK, Doot RK, Specht JM, et al. PET tumor metabolism in locally advanced breast cancer patients undergoing neoadjuvant chemotherapy: value of static versus kinetic measures of fluorodeoxyglucose uptake. *Clin Cancer Res.* 2011; 17:2400-2409.

15. Mullani NA, Herbst RS, O'Neil RG, et al. Tumor blood flow measured by PET dynamic imaging of first-pass 18F-FDG uptake: a comparison with 15O-labeled water-measured blood flow. *J Nucl Med.* 2008; 49:517-523.

16. Humbert O, Berriolo-Riedinger A, Riedinger JM, et al. Changes in 18F-FDG tumor metabolism after a first course of neoadjuvant chemotherapy in breast cancer: influence of tumor subtypes. *Ann Oncol.* 2012; 23:2572-2577.

17. Elston CW, Ellis IO. Pathological prognostic factors in breast cancer. I. The value of histological grade in breast cancer: experience from a large study with long-term follow-up. C. W. Elston & I. O. Ellis. Histopathology 1991; 19; 403-410. *Histopathology.* 2002; 41:151-152.

18. Wolff AC, Hammond ME, Hicks DG, et al. Recommendations for human epidermal growth factor receptor 2 testing in breast cancer: American Society of Clinical Oncology/College of American Pathologists clinical practice guideline update. *J Clin Oncol.* 2013; 31:3997-4013.

19. von Minckwitz G, Untch M, Blohmer JU, et al. Definition and impact of pathologic complete response on prognosis after neoadjuvant chemotherapy in various intrinsic breast cancer subtypes. *J Clin Oncol.* 2012; 30:1796-1804.

20. Cochet A, Pigeonnat S, Khoury B, et al. Evaluation of breast tumor blood flow with dynamic first-pass 18F-FDG PET/CT: comparison with angiogenesis markers and prognostic factors. *J Nucl Med.* 2012; 53:512-520.

21. Mullani NA, Goldstein RA, Gould KL, et al. Myocardial perfusion with rubidium-82. I. Measurement of extraction fraction and flow with external detectors. *J Nucl Med.* 1983; 24:898-906.

22. Berriolo-Riedinger A, Touzery C, Riedinger JM, et al. [18F]FDG-PET predicts complete pathological response of breast cancer to neoadjuvant chemotherapy. *Eur J Nucl Med Mol Imaging.* 2007; 34:1915-1924.

23. Humbert O, Cochet A, Riedinger JM, et al. HER2-positive breast cancer: F-FDG PET for early prediction of response to trastuzumab plus taxane-based neoadjuvant chemotherapy. *Eur J Nucl Med Mol Imaging.* 2014; 41:1525-1533.

24. Hanahan D, Weinberg RA. Hallmarks of cancer: the next generation. *Cell.* 2011; 144:646-674.

25. Gerber B, Loibl S, Eidtmann H, et al. Neoadjuvant bevacizumab and anthracycline-taxane-based chemotherapy in 678 triple-negative primary breast cancers; results from the geparquinto study (GBG 44). *Ann Oncol.* 2013; 24:2978-2984.

26. Kumler I, Christiansen OG, Nielsen DL. A systematic review of bevacizumab efficacy in breast cancer. *Cancer Treat Rev.* 2014; 40:960-973.

27. Miller JC, Pien HH, Sahani D, Sorensen AG, Thrall JH. Imaging angiogenesis: applications and potential for drug development. *J Natl Cancer Inst.* 2005; 97:172-187.

28. Pickles MD, Lowry M, Manton DJ, Turnbull LW. Prognostic value of DCE-MRI in breast cancer patients undergoing neoadjuvant chemotherapy: a comparison with traditional survival indicators. *Eur Radiol.* 2015; 25:1097-1106.

29. Li SP, Makris A, Beresford MJ, et al. Use of dynamic contrast-enhanced MR imaging to predict survival in patients with primary breast cancer undergoing neoadjuvant chemotherapy. *Radiology.* 2011; 260:68-78.

30. Tseng J, Dunnwald LK, Schubert EK, et al. 18F-FDG kinetics in locally advanced breast cancer: correlation with tumor blood flow and changes in response to neoadjuvant chemotherapy. *J Nucl Med.* 2004; 45:1829-1837.

31. Zasadny KR, Tatsumi M, Wahl RL. FDG metabolism and uptake versus blood flow in women with untreated primary breast cancers. *Eur J Nucl Med Mol Imaging.* 2003; 30:274-280.

32. Sorlie T, Tibshirani R, Parker J, et al. Repeated observation of breast tumor subtypes in independent gene expression data sets. *Proc Natl Acad Sci U S A.* 2003; 100:8418-8423.

33. Groheux D, Giacchetti S, Delord M, et al. Prognostic impact of 18F-FDG PET/CT staging and of pathological response to neoadjuvant chemotherapy in triple-negative breast cancer. *Eur J Nucl Med Mol Imaging.* 2015; 42:377-385.

34. Tripathi C, Tewari BN, Kanchan RK, et al. Macrophages are recruited to hypoxic tumor areas and acquire a pro-angiogenic M2-polarized phenotype via hypoxic cancer cell derived cytokines oncostatin M and eotaxin. *Oncotarget.* 2014; 5:5350-5368.

35. Chambers AF, Groom AC, MacDonald IC. Dissemination and growth of cancer cells in metastatic sites. *Nat Rev Cancer.* 2002; 2:563-572.

36. Niu G, Chen X. Why integrin as a primary target for imaging and therapy. *Theranostics.* 2011; 1:30-47.

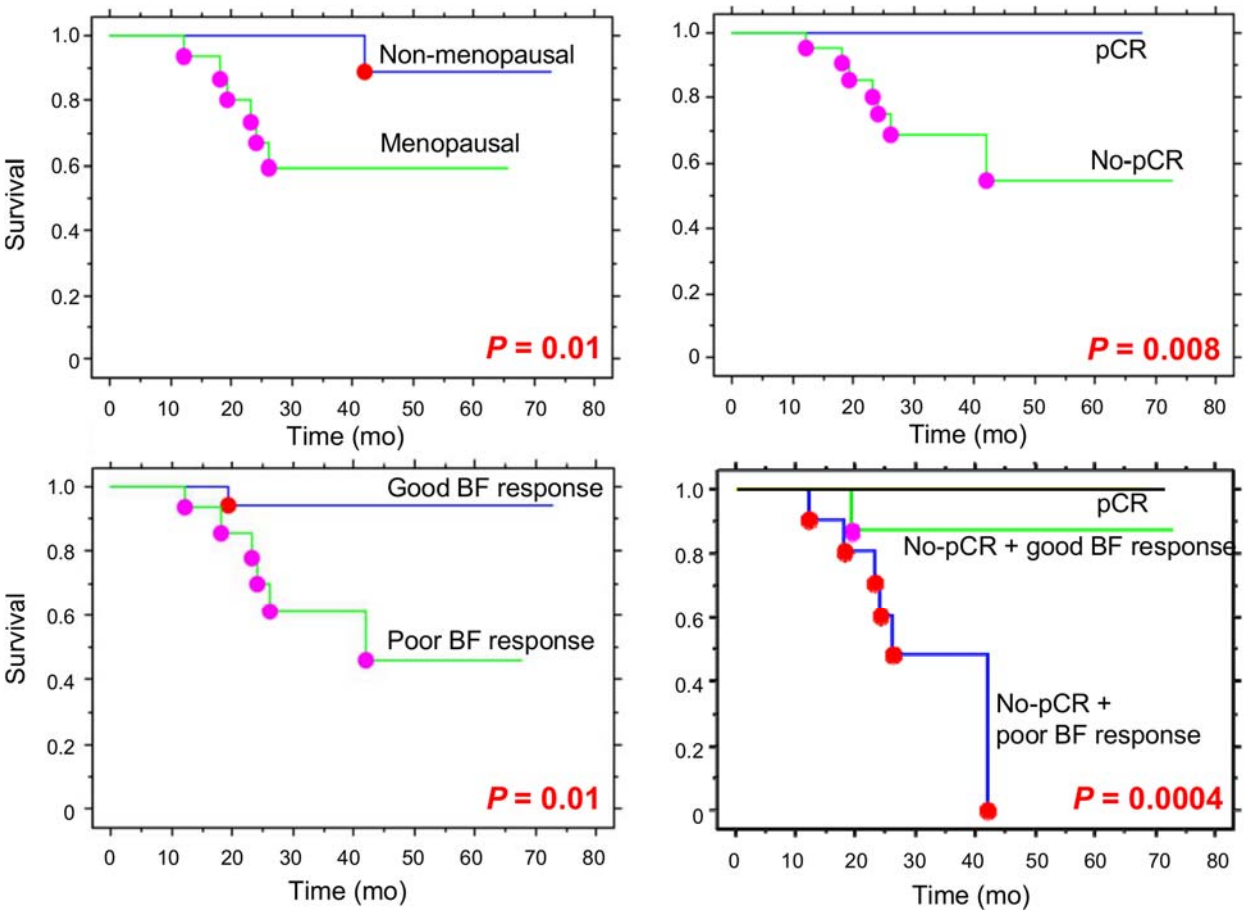

FIGURE 1. Bivariate scatterplots of tumor blood flow response (ΔBF) and tumor metabolism response (ΔSUV_{max}).

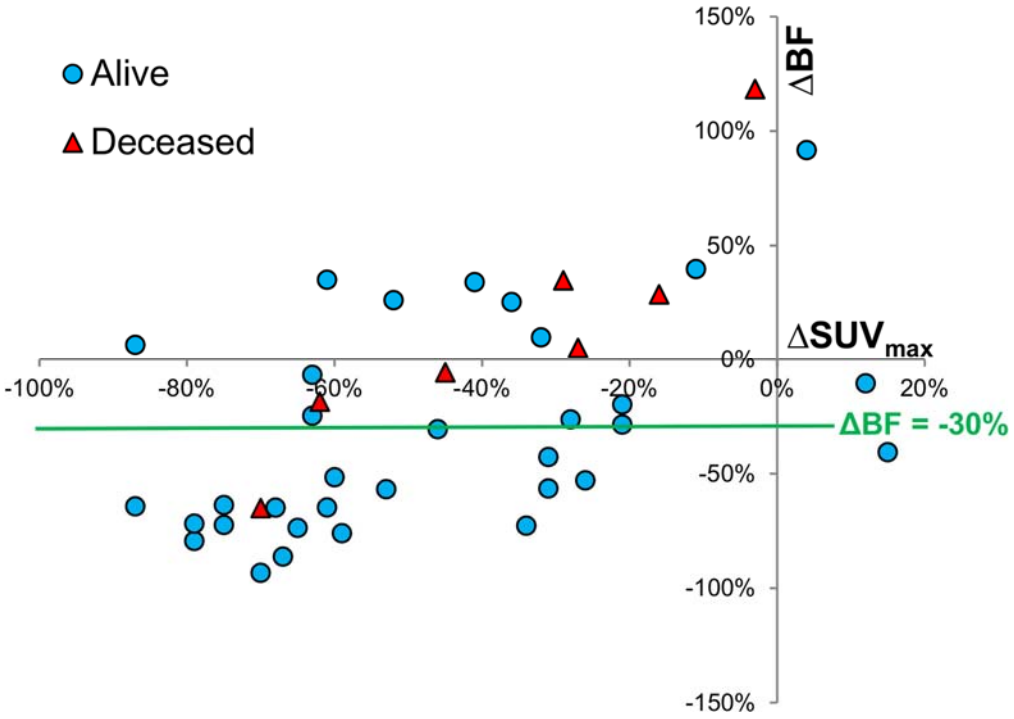

FIGURE 2. Kaplan-Meier curves showing overall survival according to menopausal status, histological response, tumor blood flow response (ΔBF cut-off= -30%), and the association of pathological response and ΔBF. *P* values were determined with Log-rank test.

TABLE 1
Factors affecting survival

Variable	Overall Survival *			Disease-Free Survival *		
	events	HR† (95% CI‡)	*P*	events	HR† (95% CI‡)	*P*
Menopausal status						
No	1/28	1		2/28	1	
Yes	6/18	9.7 [1.1-84]	**0.035**	6/18	5.4 [1.0-28]	**0.040**
Glucose metabolic response (ΔSUV_{max} cut-off = -50%)						
good metabolic response	2/20	1		2/20	1	
poor metabolic response	5/20	3.1 [0.6-16]	NS§	5/20	3.0 [0.6-16]	NS
Unknown	0/6			1/6		
BFǁ response (ΔBF cut-off = -30%)						
good BF response	1/20	1		1/20	1	
poor BF response	6/20	9.6 [1.1-84]	**0.037**	6/20	9.2 [1.1-80]	**0.040**
Unknown	0/6			1/6		
Type of surgery						
Breast-conserving	3/30	1		4/30	1	
Mastectomy	4/16	4.7 [1.0-22]	**0.046**	4/16	3.3 [0.8-14]	NS
Histological response						
pCR¶	0/20	NC#	**-**	1/20	1	
Non pCR	7/26			7/26	6.7 [0.8-57]	NS
Histological response + BF response (cut-off = -30%)						
pCR	0/20	NC	**-**	1/20	1	
Non pCR and good BF response	1/10			1/10	1.4 [0.3-20]	NS
Non pCR and poor BF response	6/13			6/13	13 [1.5-116]	**0.017**
Unknown	0/3			0/3		

* Univariate Cox proportional hazards model (patients with unknown variables were not included in the model)
† HR = hazard ratio;
‡ 95%CI = 95% confidence interval;
§ NS = Non Significant ($p > 0.05$)
ǁ BF = blood flow
¶ pCR = pathological complete response
# NC = Not calculable
Tumor size (> 5 cm), AJCC staging, lymph node involvement, history of pregnancy, SBR grading, tumor architectural differentiation, nuclear pleomorphism, number of mitosis, $SUV_{max}1$, BF_1 and the $SUV_{max}1/BF_1$ ratio were not associated with OS.